

SUPPLEMENTARY METHODS

Ethics and Enrollment

The protocol was approved by the local ethics committee of the Medical Faculty of the University of Bonn, Germany (approval no. 158/15). The study was registered in the ClinicalTrials.gov database (Identifier: NCT03421587) provided by the US National Institutes of Health. All participants gave written informed consent and the study was conducted in accordance with the latest revision of the Helsinki Declaration. Recruitment of study participants is depicted in **Figure S1**. After completion of the study, participants received monetary compensation. All behavioral and functional magnetic resonance imaging (fMRI) data were collected in Bonn, Germany.

Interpersonal Distance Paradigm

All subjects read written instructions before the experiment. A standardized appearance of the experimenter was ensured for all subjects across all sessions and all subjects were tested in the same room.

Social Touch Paradigm

Previous studies showed that the attribute *comforting* is perceived as highly emotional descriptive for the touch experience delivered at the velocities used in the social touch paradigm (1). Moreover, CT-stimulation was associated with higher comfort ratings than A-beta stimulation, rendering the perceived comfort of touch an ideal behavioral readout for the processing of CT-stimulation.

Before the fMRI experiment, a 20-cm zone was marked on each shin and during the 4 s of tactile stimulations the complete zones were covered once during slow touch (5 cm/s; CT-optimal speed) and four times during fast touch (20 cm/s; non-CT-optimal speed). The experimenter was trained in the

delivery of the tactile stimuli at both speeds maintaining constant pressure and was guided by audio cues during the experiment to ensure constant stroking velocity.

Visual cues were presented on a black backdrop using a 32-inch MRI compatible TFT LCD monitor (NordicNeuroLab, Bergen, Norway) placed at the rear of the magnet bore using Presentation 14 (Neurobehavioral Systems, Albany, CA, USA). Participants made their responses using an MRI-compatible response grip system (NordicNeuroLab AS, Bergen, Norway). Two buttons were used to move the cursor left and right on the visual analogue scale and participants confirmed their responses by pressing either of these buttons. Participants learned the button press coding before the scan.

Physiological Data Acquisition

Physiological data were recorded throughout the fMRI paradigm using a Biopac MP150 system and the accompanying AcqKnowledge Acquisition & Analysis Software (Version 4.3.1) applying a sampling frequency of 1000 Hz. Respiratory signal was recorded via an MR-compatible breathing belt (RX-TSD221-MRI) affixed to the subject's chest to record thoracic contraction and expansion. The breathing belt was connected to a differential pressure transducer in the monitoring room via a 1.5 mm MR-compatible tube (AFT30-XL) with a length of 10 m. Noise was removed using hardware-based filters included in the amplifier with a low-pass filter of 1 Hz and a high-pass filter of 0.05 Hz. Blood volume pulse signal was recorded with an MR-compatible photoplethysmogram (PPG) transducer (TSD200-MRI) attached to the tip of the subject's right long toe. The PPG transducer was connected to a PPG amplifier (PPG100C) placed in the monitoring room via a 3 m shielded cable. A hardware-based low-pass filter of 3 Hz and a high-pass filter of 0.5 Hz were applied to the PPG signal for noise removal.

fMRI Data Acquisition

A Siemens MAGNETOM Trio MRI system (Siemens, Erlangen, Germany) operating at 3T and equipped with a 32-channel phased-array head coil (Siemens, Erlangen, Germany) was used to acquire T2*-weighted echoplanar (EPI) images with blood-oxygen-level-dependent contrast (TR = 2690 ms, TE = 30 ms, pixel size: 2 x 2 x 3 mm, slice thickness = 3.0 mm, distance factor = 10 %, FoV = 192 mm, flip angle =

90°, 41 axial slices). High-resolution anatomical images were obtained on the same scanner using a T1-weighted 3D MPRAGE sequence (imaging parameters: TR = 1660 ms, TE = 2.54 ms, matrix size: 256 x 256, pixel size: 0.8 x 0.8 x 0.8 mm, slice thickness = 0.8 mm, FoV = 256 mm, flip angle = 9°, 208 sagittal slices).

fMRI Data Analysis

The MRI data were preprocessed and analyzed using SPM12 software (Wellcome Trust Centre for Neuroimaging, London, United Kingdom; <http://www.fil.ion.ucl.ac.uk/spm>) implemented in MATLAB R2010b (MathWorks, Natick, Massachusetts, USA). The first five volumes of each functional time series were discarded to allow for T1 equilibration. Images were corrected for head movement between scans by an affine registration. For realignment, a two-pass procedure was used by which images were initially realigned to the first image of the time series and subsequently re-realigned to the mean of all images. For normalization, a two-step procedure was applied. Normalization parameters were first determined by segmenting the T1-image using the default tissue probability maps. Next, normalization parameters were applied to normalize the functional images to the standard anatomical Montreal Neurological Institute (MNI) space resampled at 2 × 2 × 2 mm voxel. The normalized images were spatially smoothed using a 6-mm FWHM Gaussian kernel. Raw time series were detrended using a high-pass filter (cut-off period, 128 s).

On the first level, onsets and durations of the five experimental conditions ('Slow Touch_{Announced}', 'Slow Touch_{Unannounced}', 'Fast Touch_{Announced}', 'Fast Touch_{Unannounced}', 'No Touch') were modeled by a stick function convolved with a hemodynamic response function in the context of a general linear model. Furthermore, we performed model-based physiological noise correction using the PhysIO toolbox (2). For this purpose, we computed RETROICOR (retrospective image correction) (3) regressors, applying a 3rd order cardiac, 4th order respiratory, and 1st order interaction Fourier expansion of cardiac and respiratory phase (4), as well as RVT (respiratory volume per time) (5) regressors. The resulting 19 physiological noise regressors as well as the six regressors for realignment parameters were included as confounds in the design matrix. For each participant, contrast images were generated in each individual random-effects

first-level analysis comparing condition-specific activation relative to low level baseline.

On the second level, to compute the main contrasts of interest [(low $CM_{Slow>Fast}$ > high $CM_{Slow>Fast}$)] and [(high $CM_{Slow>Fast}$ > low $CM_{Slow>Fast}$)], contrast images were entered into a 3×2 flexible factorial design with childhood maltreatment (CM) level group (low CM, medium CM, high CM) as a between-subject factor, touch velocity (slow, fast) as within-subject factor and the BOLD response to social touch as dependent variable. To explore potential further differences of social touch responsiveness between the three subject groups, we also computed the contrasts [(low $CM_{Slow>Fast}$ > medium $CM_{Slow>Fast}$)], [(medium $CM_{Slow>Fast}$ > low $CM_{Slow>Fast}$)], [(medium $CM_{Slow>Fast}$ > high $CM_{Slow>Fast}$)] and [(high $CM_{Slow>Fast}$ > medium $CM_{Slow>Fast}$)]. We also conducted an analysis with separate regressors for announced and unannounced touch trials (i.e. CM group as between-subject factor, announcement (announced, unannounced) as within-subject factor and the BOLD response for the contrast (Slow>Fast) as dependent variable), but in line with the behavioral results, fMRI analysis did not reveal significant interactions between touch announcement, touch velocity and CM. Thus, for our main fMRI analysis, the within-subject factor touch velocity was averaged across both levels of touch announcement. Furthermore, we also assessed CM as a continuous variable and examined the effect of social touch by calculating two random-effects regression models using the BOLD-responses to the contrasts [(Slow Touch)] and [(Fast Touch)] as dependent variables (see **Supplementary Results**). Task-specific effects [(Slow Touch > Fast Touch)], [(Fast Touch > Slow Touch)] and social touch activation [(Touch > No Touch)], [(No Touch > Touch)] were investigated in the low CM subject group in a region of interest (ROI) approach and at the whole-brain level applying a height threshold of $P < 0.001$ (uncorrected) (see **Table S4**). The main fMRI and VBM analysis focused on a set of a priori bilateral ROIs consisting of the amygdala, hippocampus, insula and SI, which were anatomically defined according to the Wake Forest University Pick Atlas (Version 3.0). P -values were corrected for multiple comparisons (family-wise error (FWE)) and $P < 0.05$ was considered significant. P -values of the whole-brain analyses are reported at the peak-level (6). The anatomical labeling for the whole-brain data was performed by means of the AAL-Toolbox (<http://www.gin.cnrs.fr/AAL>) (7). To explore possible differential effects of the control condition, we compared the BOLD-response to the contrast [(No Touch)] between all three CM groups. For further

statistical analyses, parameter estimates were extracted from significant clusters of the BOLD level analysis using the Marsbar Toolbox and gray matter volume (GMV) values were extracted from the significant clusters of the region-specific VBM analysis using the get_totals script (<http://www.nemotos.net/?p=292>).

Voxel-Based Morphometry

The GMV data were analyzed in SPM12 using an absolute threshold masking of 0.1. All T1-weighted images were corrected for bias-field inhomogeneities, tissue classified and spatially normalized to MNI-space at a voxel size of $1.5 \times 1.5 \times 1.5 \text{ mm}^3$ using the diffeomorphic anatomical registration through exponentiated lie algebra (DARTEL) algorithm (8). Homogeneity of gray matter images was checked using the covariance structure of each image with all other images, as implemented in the check data quality function. In addition to visual inspections, all scans passed the automated data quality check protocol. Subsequently, the modulated GMV images were smoothed with an isotropic Gaussian kernel of 8 mm full width half maximum (FWHM).

Given our a priori directional hypothesis on GMV reductions after CM based on previous work (9) (10), we specifically contrasted CM groups computing the contrasts ([low CM > high CM]), ([low CM > medium CM]) and ([medium CM > high CM]). The anatomical labeling for the whole-brain data was performed by means of the AAL-Toolbox (<http://www.gin.cnrs.fr/AAL>) (7).

Statistical Analysis

Behavioral, demographic and psychometric data were analyzed using SPSS version 24 (IBM Corp., Armonk, NY, USA). Quantitative behavioral data were compared by mixed analyses of variance (ANOVAs), one-way between-subject ANOVAs and independent *t*-tests. Pearson's product-moment correlation was used for correlation analysis. Partial eta-squared and Cohen's *d* were calculated as measures of effect size. Possible sociodemographic and psychometric a priori differences between the three CM level groups were explored using Pearson's chi-squared tests and one-way between-subjects ANOVAs. Fisher's *r*-to-*z* transformation was used for the comparison of correlation coefficients. Reported

P-values are one-tailed for directional post hoc statistics and two-tailed for all other analyses. Post-hoc *t*-tests were Bonferroni-corrected to account for multiple comparisons.

Mediation and Moderation Analysis

Mediation and moderation analyses were performed using the PROCESS macro for SPSS version 3.1 (11), with the social touch ratings and the parameter estimates extracted from significant clusters serving as the criterion variables. All covariates were assessed individually in separate moderation and mediation models. Heteroscedasticity-consistent standard errors were used for all analyses and mean-centering was used in the analyses for interaction effects. The significance of indirect effects was examined using 95% bootstrapped (10 000 bootstrap samples) symmetric confidence intervals (95% CIs). Indirect effects were considered significant when the upper and lower bound of 95% CI did not contain zero. However, since the underlying mediation framework of PROCESS does not support dichotomous mediators, we explored a potential mediation effect of gender by employing the Baron and Kenny four steps regression approach (12). Moderation was assumed when the interaction term between the predictor variable CM and a moderation variable was significant. In addition, the Johnson-Neyman technique was applied to the conditional effects to probe these associations and identify the threshold of significance. For these analyses, the level of statistical significance was set at $P < 0.05$ and all reported *P* values are two-tailed.

SUPPLEMENTARY RESULTS

Subjects

We screened a total of 120 subjects for the present study (see **Figure S1**). Fifteen subjects had to be excluded due to medication intake at the time of the screening. Five subjects had to be excluded due to discontinuation of study participation. Furthermore, three subjects had to be excluded due to MRI contraindications. Another five subjects were excluded due to psychotic disorders diagnosed by an experienced psychologist using the German version of the Structured Clinical Interview for DSM-IV (13) in the screening session.

Missing Values

One participant of the medium CM group did not participate in the stop-distance experiment. Scores of Clinician-Administered PTSD Scale (14) were not recorded for one participant of the low CM group. Due to technical malfunctions of the online questionnaire software during the screening sessions, the Social Touch Questionnaire (15) and the Perceived Stress Scale (16) could not be administered to two participants of the low CM group and one participant of the medium CM group.

Prevalence of Trauma Type

In total, 42.4 % of the study sample had experienced multi-type maltreatment during childhood. Prevalence rates for each subtype of maltreatment (emotional abuse, physical abuse, sexual abuse, emotional neglect, physical neglect) within the current study sample are reported in **Table S2**. For each subscale of the Childhood Trauma Questionnaire (CTQ), slight-to-severe cut-off scores by Bernstein et al. (17) were used to classify a history of childhood maltreatment (CM). This classification has also been used in previous reports on CM in Germany (18). Subjects with CTQ scores below these thresholds reported either no or mild experiences of CM. Subjects' reported maltreatment experiences included verbal abuse, being terrorized with threats, affective deprivation or lack of affection, beating, being pelted with objects and having been looked up for longer periods of time, parental substance and/or alcohol

abuse, molestation, rape and parental kidnapping as assessed by the Clinician-Administered PTSD Scale (19).

Behavioral Results

A 2×3 mixed ANOVA with the within-subject factor social distance (ideal, uncomfortable) and the CM group as a between-subject factor (low CM, medium CM, and high CM) yielded a main effect of social distance ($F_{(1,88)} = 18.28$, $P < 0.001$, $\eta p^2 = 0.17$), but no other significant main or interaction effects (all P s > 0.05). However, an exploratory one-way ANOVA for the ideal distance showed a trend-to-significant difference between low, medium, and high CM levels ($F_{(2,88)} = 2.65$, $P = 0.076$, $\eta p^2 = 0.06$). The uncomfortable distance did not significantly differ between the three CM groups ($P = 0.34$).

Consistent with our main behavioral results, a supplemental regression analysis showed that higher CM levels predicted larger ideal social distances ($\beta = 0.30$, $P = 0.004$), with 9% of the variation explained by the model ($R^2 = 0.09$, $F_{(1,89)} = 8.76$, $P = 0.004$), whereas CM did not predict the uncomfortable social distances ($P = 0.26$). Moreover, a second regression analysis revealed that participants with higher CM levels perceived fast touch stimulations as less comforting ($\beta = -0.41$, $P < 0.001$), with 16.6 % of the variation explained by the model ($R^2 = 0.17$, $F_{(1,91)} = 17.87$, $P < 0.001$), whereas CM did not predict the perceived comfort of slow touch stimulations ($P = 0.69$). An additional one-way between-subject ANOVA showed that there were no significant differences between CM groups for the No Touch control condition ($P = 0.26$).

Moreover, we observed a significant negative correlation between loss of sexual interest as measured by Beck's Depression Inventory (item 21) and comfort ratings of fast touch ($r_{(92)} = -0.28$, $P = 0.01$, but not slow touch ($P = 0.98$). As such, CM-associated dysregulation of fast touch processing may negatively affect relationship quality.

fMRI Results

The fMRI analysis showed no significant higher order interaction of announcement, touch velocity and CM group (all P s > 0.05). However, we observed a main effect of touch announcement at the whole-brain level, evident in significantly increased responses to announced touch relative to unannounced touch in the right inferior occipital lobe (peak MNI coordinates x, y, z : 26, -96; -2, $t_{(164)} = 5.16$, $P_{FWE} = 0.022$) and the right inferior temporal gyrus (40, -50, -4; $t_{(164)} = 5.08$, $P_{FWE} = 0.031$). The analysis yielded no significant main effect of announcement in our a priori ROIs (all P s > 0.05). Furthermore, there were no significant differences between CM groups for the No Touch control condition (all P s > 0.05).

Complementary regression analysis showed that higher CM levels were associated with lower limbic responsiveness to slow touch in the right hippocampus (peak MNI coordinates x, y, z : 36, -12, -24; $t_{(83)} = 3.67$, $P_{FWE} = 0.039$) and the right amygdala (24, 2, -20; $t_{(83)} = 3.53$, $P_{FWE} = 0.015$) and with increased cortical reactivity in the right insula (38, -18, 6; $t_{(83)} = 4.36$, $P_{FWE} = 0.008$) and a trend-to-significant increased activation in the right somatosensory cortex (42, -22, 60; $t_{(83)} = 3.95$, $P_{FWE} = 0.055$) to fast touch.

Voxel-Based Morphometry Results

Subjects with high levels of CM also exhibited reduced GMV in the bilateral hippocampus (27, -21, -11; $t_{(76)} = 4.77$, $P_{FWE} < 0.001$; -23, -21, -12; $t_{(76)} = 6.25$, $P_{FWE} < 0.001$), amygdala (36, 0, -24; $t_{(76)} = 5.23$, $P_{FWE} < 0.001$; -23, -5, -26; $t_{(76)} = 5.25$, $P_{FWE} < 0.001$), somatosensory cortex (-56, -18, 32; $t_{(76)} = 4.04$, $P_{FWE} = 0.017$; 54, -27, 48; $t_{(76)} = 3.80$, $P_{FWE} = 0.034$) and in the left insula (-44, -3, 0; $t_{(76)} = 4.91$, $P_{FWE} < 0.001$) relative to subjects with a medium level of CM. Thus, subjects with a high level of CM exhibited significantly decreased region-specific GMV compared to subjects with low and medium levels of CM.

Effect of Trauma Type

The five CTQ subscales were significantly intercorrelated due to the fact that several participants had experienced multiple traumas. We observed the strongest associations between physical and emotional neglect ($r_{(92)} = 0.79$, $P < 0.001$), followed by emotional neglect and emotional abuse ($r_{(92)} = 0.78$, $P <$

0.001), emotional neglect and physical abuse ($r_{(92)} = 0.72, P < 0.001$), emotional abuse and physical abuse ($r_{(92)} = 0.71, P < 0.001$), and physical neglect and emotional abuse ($r_{(92)} = 0.66, P < 0.001$).

However, the subscale sexual abuse showed the weakest association with all the other subscales as only a few subjects of the sample reported sexual abuse exposure during childhood with smaller associations between sexual abuse and physical abuse ($r_{(92)} = 0.26, P = 0.012$), sexual abuse and physical neglect ($r_{(92)} = 0.3, P = 0.004$), sexual abuse and emotional neglect ($r_{(92)} = 0.29, P = 0.005$) and sexual abuse and emotional abuse ($r_{(92)} = 0.25, P = 0.015$).

All CTQ subscales negatively correlated with the comfort ratings of fast touch (emotional abuse $r_{(92)} = -0.38, P < 0.01$; physical abuse $r_{(92)} = -0.31, P < 0.01$; sexual abuse $r_{(92)} = -0.22, P = 0.04$; emotional neglect $r_{(92)} = -0.39, P < 0.01$; physical neglect $r_{(92)} = -0.30, P < 0.01$). Likewise, all CTQ subscales showed significant or trend-to-significant positive correlation with parameter estimates of neural responses to fast touch in the somatosensory cortex touch (emotional abuse $r_{(85)} = 0.29, P < 0.01$; physical abuse $r_{(85)} = 0.22, P = 0.04$; sexual abuse $r_{(85)} = 0.25, P = 0.02$; emotional neglect $r_{(85)} = 0.35, P < 0.01$; physical neglect $r_{(85)} = 0.21, P = 0.06$) and posterior insula (emotional abuse $r_{(85)} = 0.21, P = 0.06$; physical abuse $r_{(85)} = 0.20, P = 0.06$; sexual abuse $r_{(85)} = 0.45, P < 0.01$; emotional neglect $r_{(85)} = 0.25, P = 0.02$; physical neglect $r_{(85)} = 0.26, P = 0.02$). Significant or trend-to-significant positive correlations between comfort ratings of slow touch and parameter estimates of hippocampus responses to slow touch were only evident for physical abuse ($r_{(85)} = -0.23, P = 0.03$) and emotional neglect ($r_{(85)} = -0.21, P = 0.06$; other P s $> .12$). However, conversion of correlation coefficients into z-scores by Fisher's r -to- z transformation (20) revealed that the correlation coefficients did not significantly differ between CTQ subscales after correction for multiple comparisons.

SUPPLEMENTAL TABLES

Table S1. Distribution of lifetime psychiatric disorders within the sample

Psychiatric Disorder	Number of Lifetime Diagnoses		
	CTQ Low	CTQ Medium	CTQ High
Depressive Disorders	3	7	18
Anxiety Disorders	1	2	13
Post-traumatic Stress Disorder	0	1	6
Obsessive-compulsive Disorder	0	1	3
Eating Disorders	1	0	3
Alcohol Abuse / Dependency	0	1	5
Substance Abuse / Dependency	0	1	1
Personality Disorders	0	0	5

Notes. Lifetime psychiatric disorders were diagnosed using the German version of the Structured Clinical Interviews for DSM-IV. The Clinician-Administered PTSD Scale (CAPS) was used for diagnosing and measuring the severity of current PTSD.

Table S2. Exposure to childhood maltreatment type and frequencies

	%
Emotional Abuse	39.1
Physical Abuse	22.8
Sexual Abuse	19.6
Emotional Neglect	47.8
Physical Neglect	34.8
Any CM Type	60.9
Exposure to 1 CM Type	18.5
Exposure to ≥ 2 CM Type	42.4

Notes. History of childhood maltreatment included all reports of slight to extreme childhood maltreatment exposure on at least one subdomain of childhood maltreatment based on the classification of Bernstein et al. (17). Abbreviations: CM, childhood maltreatment.

Table S3. Demographic and psychometric sample characteristics

	Low CM (n = 33)	Medium CM (n = 30)	High CM (n=29)	χ^2 / F	P
Age (years)	25.7 ± 0.97	29.53 ± 1.97	28.35 ± 1.56	1.72	0.19
Sex (F/M)	24/9	16/14	24/5	6.27	0.04
Education (years)	16.4 ± 0.59	15.69 ± 0.56	15.95 ± 0.68	0.36	0.7
CTQ Score	26.61 ± 0.28	35.53 ± 0.67	63.35 ± 2.61	165.18	<0.001
CTQ Emotional Neglect	6.03 ± 0.23	9.37 ± 0.47	16.9 ± 0.89	93.72	<0.001
CTQ Emotional Abuse	5.23 ± 0.09	8.17 ± 0.54	16.24 ± 0.95	88.38	<0.001
CTQ Physical Abuse	5.03 ± 0.03	5.3 ± 0.11	10.59 ± 0.75	56.42	<0.001
CTQ Physical Neglect	5.27 ± 0.13	7 ± 0.4	10.9 ± 0.69	41.65	<0.001
CTQ Sexual Abuse	5 ± 0	5.7 ± 0.39	8.72 ± 1.06	10.02	<0.001
CAPS-5	3.19 ± 1.49	5.93 ± 1.36	16.48 ± 2.28	16.25	<0.001
BDI	4.49 ± 1.07	8.2 ± 1.28	22.59 ± 2.65	29.38	<0.001
PSS	11.23 ± 1.05	17.41 ± 1.11	21.97 ± 1.27	22.65	<0.001
Social Touch Aversion	24.61 ± 1.41	32.45 ± 1.76	35.59 ± 2.33	9.46	<0.001

Notes. Values are given as mean ± standard error. Subjects (n = 92 in the behavioral analysis) were stratified into low, medium and high levels of childhood maltreatment (CM) exposure by means of a tertile split of Childhood Trauma Questionnaire (CTQ) sum scores. Abbreviations: CM, Childhood maltreatment; CTQ, Childhood Trauma Questionnaire; CAPS-5, Clinician-Administered PTSD Scale for DSM-5; BDI, Beck Depression Inventory; PSS, Perceived Stress Scale.

Table S4. Activation table for GLM analysis of social touch velocity (slow vs. fast) in the low CM group

Region	Right/left	<i>t</i> -score	<i>MNI Coordinates</i>			<i>P</i>
			<i>x</i>	<i>y</i>	<i>z</i>	
Slow Touch > Fast Touch						
Anterior Cingulate Cortex	R	5.67	12	48	18	<0.001
Angular Gyrus	L	4.85	-44	-64	24	<0.001
Anterior Cingulate Cortex	R	4.66	8	22	20	<0.001
Fusiform Gyrus	R	4.63	40	-16	-24	<0.001
Insula	L	4.50	-32	2	14	<0.001
Insula	R	4.28	38	8	10	<0.001
Middle Temporal Gyrus	L	4.23	-62	-14	-18	<0.001
Superior Temporal Pole	R	4.05	44	8	-26	<0.001
Inferior Frontal Gyrus, Pars Triangularis	R	4.00	48	28	8	<0.001
Inferior Frontal Gyrus, Pars Triangularis	L	3.96	-34	28	12	<0.001
Posterior Cingulate Cortex	L	3.93	-4	50	32	<0.001
Inferior Temporal Gyrus	L	3.88	-44	-22	-20	<0.001
Middle Frontal Gyrus	L	3.76	-20	28	36	<0.001
Fusiform Gyrus	L	3.70	-40	-46	-20	<0.001
Rolandic Operculum	R	3.69	50	-8	14	<0.001
Fusiform Gyrus	R	3.66	38	-40	-20	<0.001
Superior Temporal Pole	L	3.57	-36	16	-28	<0.001
Middle Cingulate Cortex	L	3.48	-18	-14	42	<0.001
Rolandic Operculum	R	3.46	56	8	0	<0.001
Supramarginal Gyrus	L	3.45	-54	-28	28	<0.001
Anterior Cingulate Cortex	R	3.45	12	42	0	<0.001
Middle Cingulate Cortex	R	3.44	10	-2	30	<0.001
Insula	R	3.40	40	0	20	<0.001
Transverse Temporal Gyrus	R	3.40	52	-12	6	<0.001
Superior Temporal Pole	L	3.40	-30	4	-26	<0.001
Supramarginal Gyrus	R	3.39	62	-26	26	<0.001
Supramarginal Gyrus	R	3.32	40	-32	28	0.001
Anterior Cingulate Cortex	L	3.30	-4	-2	28	0.001
Superior Parietal Lobule	R	3.26	16	-50	68	0.001
Medial Frontal Gyrus	L	3.26	-10	46	20	0.001

Putamen	L	3.24	-12	6	-8	0.001
Middle Temporal Gyrus	L	3.24	-54	-14	-8	0.001
Inferior Frontal Gyrus, Pars Triangularis	R	3.23	38	30	12	0.001
Inferior Temporal Gyrus	R	3.22	46	-48	-14	0.001
Inferior Frontal Gyrus, Pars Triangularis	L	3.21	-40	26	6	0.001
Middle Frontal Gyrus	L	3.19	-28	46	28	0.001
Fusiform Gyrus	L	3.18	-34	-14	-24	0.001
Rolandic Operculum	R	3.18	60	-2	10	0.001
Paracentral Lobule	R	3.15	20	-42	50	0.001
Superior Temporal Gyrus	L	3.15	-56	-10	-6	0.001
Putamen	L	3.15	-34	-10	0	0.001
Inferior Frontal Gyrus, Pars Orbitalis	L	3.14	-38	32	-4	0.001
Middle Temporal Gyrus	R	3.13	52	-12	-12	0.001
Superior Temporal Pole	L	3.13	-28	8	-26	0.001
Hippocampus	L	3.13	-32	-16	-22	0.001
Middle Cingulate Cortex	R	3.13	14	-28	30	0.001
Fast Touch > Slow Touch						
Supplementary Motor Area	R	4.53	20	-20	52	<0.001
Inferior Frontal Gyrus, Pars Triangularis	R	4.23	48	30	30	<0.001
Superior Temporal Gyrus	L	4.14	-60	-38	14	<0.001
Inferior Frontal Gyrus, Pars Orbitalis	R	3.68	42	8	-2	<0.001
Cerebellum IV V	L	3.68	-4	-50	-2	<0.001
Superior Frontal Gyrus	R	3.55	30	14	62	<0.001
Inferior Frontal Gyrus, Pars Orbitalis	L	3.44	-22	46	-4	<0.001
Frontal Superior Gyrus	R	3.20	20	12	46	0.001
Frontal Superior Gyrus	L	3.20	-12	32	42	0.001
Hippocampus	L	3.13	-22	-40	6	0.001

Notes. For the whole-brain analysis a height threshold of $P < 0.001$ (uncorrected) was used. P -values are reported at peak level. Task effects were explored in subjects with a low level of experienced childhood maltreatment.

Table S5. Results of the Whole Brain Voxel-based Morphometry Analysis

Region	Right/left	<i>t</i> -score	MNI Coordinates			<i>P</i>
			<i>x</i>	<i>y</i>	<i>z</i>	
Low CM > High CM						
Gyrus Rectus	R	7.24	5	21	20	<0.001
Middle Temporal Gyrus	R	6.01	66	-39	6	<0.001
Insula	L	5.77	-38	-15	12	<0.001
Fusiform Gyrus	R	5.77	38	39	-14	<0.001
Inferior Frontal Gyrus, Pars Triangularis	R	4.92	53	35	18	<0.001
Inferior Occipital Gyrus	L	4.84	-57	-69	12	<0.001
Middle Occipital Gyrus	L	4.57	-24	-80	38	<0.001
Middle Temporal Gyrus	R	4.53	56	-72	17	<0.001
Precentral Gyrus	L	4.39	-44	8	44	<0.001
Fusiform Gyrus	L	4.34	-35	-33	-24	<0.001
Precuneus	R	4.29	6	-74	41	<0.001
Lingual Gyrus	L	4.21	-14	-78	-11	<0.001
Cerebellum VIII	R	4.18	38	-45	-57	<0.001
Fusiform Gyrus	R	4.14	33	-75	-17	<0.001
Cuneus	R	4.12	6	-90	33	<0.001
Lingual Gyrus	R	4.11	11	-72	-3	<0.001
Middle Cingulate Cortex	R	4.06	2	-30	47	<0.001
Middle Temporal Pole	R	4.01	23	5	-41	<0.001
Fusiform Gyrus	L	3.99	-27	-3	-51	<0.001
Superior Occipital Gyrus	R	3.90	27	-75	39	<0.001
Cerebellum VIII	L	3.85	-6	-66	-59	<0.001
Superior Occipital Gyrus	R	3.81	23	-93	3	<0.001
Supramarginal Gyrus	L	3.81	-62	-39	26	<0.001
Insula	L	3.79	-38	2	20	<0.001
Crus Cerebellum II	R	3.79	51	-54	-50	<0.001
Cuneus	R	3.77	2	-96	17	<0.001
Inferior Temporal Gyrus	R	3.73	63	-56	-17	<0.001
Superior Temporal Gyrus	L	3.70	-48	-42	15	<0.001
Inferior Frontal Gyrus, Pars Orbitalis	R	3.60	53	44	-12	<0.001

Inferior Frontal Gyrus, Pars Triangularis	R	3.59	59	30	3	<0.001
Thalamus	L	3.53	-14	-27	18	<0.001
Precuneus	R	3.52	-14	-14	36	
Precuneus	L	3.51	-8	-47	51	<0.001
Middle Temporal Gyrus	R	3.51	68	-51	-8	<0.001
Middle Temporal Gyrus	R	3.46	65	-59	3	<0.001
Inferior Temporal Gyrus	R	3.42	45	-44	-21	<0.001
Middle Occipital Gyrus	L	3.42	-47	-84	17	0.001
Inferior Temporal Gyrus	R	3.42	51	-44	-15	0.001
Inferior Frontal Gyrus, Pars Triangularis	R	3.39	41	38	2	0.001
Superior Frontal Gyrus	R	3.38	26	27	51	0.001
Middle Frontal Gyrus	R	3.36	41	27	53	0.001
Supplementary Motor Area	L	3.34	-8	25	57	0.001
Angular Gyrus	L	3.33	-51	-77	26	0.001
Fusiform Gyrus	L	3.33	-30	-56	-12	0.001
Angular Gyrus	L	3.33	-54	-65	30	0.001
Inferior Frontal Gyrus, Pars Orbitalis	R	3.32	41	51	-15	0.001
Middle Frontal Gyrus	L	3.31	-39	44	35	0.001
Middle Frontal Gyrus	L	3.30	-45	54	8	0.001
Rolandic Operculum	R	3.29	42	6	14	0.001
Superior Frontal Gyrus	L	3.28	-17	35	59	<0.001
Calcerine Sulcus	L	3.28	-14	-54	12	<0.001
Inferior Frontal Gyrus, Pars Orbitalis	R	3.27	51	30	-14	<0.001
Inferior Frontal Gyrus, Pars Orbitalis	R	3.27	35	33	-8	<0.001
Superior Temporal Pole	R	3.27	42	27	-23	<0.001
Cerebellum VIII	R	3.26	6	-68	-57	0.001
Angular Gyrus	L	3.25	-51	-78	23	0.001
Cerebellum IX	R	3.25	3	-65	-51	0.001
Thalamus	R	3.24	5	-23	14	0.001
Middle Temporal Gyrus	R	3.23	68	-53	-5	0.001
Precentral Gyrus	L	3.23	-50	12	32	0.001

Inferior Temporal Gyrus	R	3.22	60	-62	-15	0.001
Superior Frontal Gyrus	L	3.22	-14	71	11	0.001
Middle Frontal Gyrus, Pars Orbitalis	R	3.20	36	57	-14	0.001
Medial Orbitofrontal Cortex	R	3.20	-9	71	8	0.001

Medium CM > High CM

Insula	R	7.49	50	-6	5	<0.001
Middle Cingulum Cortex	R	5.23	6	-26	39	<0.001
Cerebellum III	R	5.10	18	-29	-32	<0.001
Inferior Parietal Lobule	R	4.85	48	-45	50	<0.001
Precuneus	L	4.75	-9	-60	-32	<0.001
Superior Frontal Gyrus	R	4.48	20	26	48	<0.001
Inferior Parietal Lobule	L	4.39	-32	-72	44	<0.001
Inferior Frontal Gyrus, Pars Orbitalis	R	4.31	39	41	-8	<0.001
Postcentral Gyrus	L	4.19	-48	-18	29	<0.001
Cuneus	R	4.17	6	-90	33	<0.001
Precuneus	L	3.99	-15	-53	50	<0.001
Middle Frontal Gyrus	L	3.91	-27	18	56	<0.001
Inferior Temporal Gyrus	R	3.90	51	-44	-15	<0.001
Cuneus	R	3.83	21	-72	33	<0.001
Middle Frontal Gyrus	L	3.82	-29	20	42	<0.001
Supplementary Motor Area	L	3.81	-8	-2	57	<0.001
Lingual Gyrus	L	3.80	-18	-65	-2	<0.001
Calcerine Sulcus	L	3.78	-17	-72	15	<0.001
Middle Frontal Gyrus	L	3.77	-27	35	45	<0.001
Superior Parietal Lobule	L	3.66	-20	-62	59	<0.001
Supramarginal Gyrus	L	3.65	-56	-38	26	<0.001
Middle Frontal Gyrus	R	3.64	45	11	56	<0.001
Calcerine Sulcus	R	3.60	3	-98	-5	<0.001
Inferior Frontal Gyrus, Pars Triangularis	R	3.58	42	32	26	<0.001
Lingual Gyrus	L	3.55	-11	-90	-17	<0.001
Supramarginal Gyrus	L	3.54	-15	29	39	<0.001
Cuneus	R	3.47	2	-96	18	<0.001
Supramarginal Gyrus	R	3.46	54	-24	32	<0.001

Superior Occipital Gyrus	R	3.45	24	-72	20	<0.001
Calcerine	R	3.45	21	-93	2	<0.001
Crus Cerebellum I	L	3.44	-41	-47	-38	<0.001
Inferior Temporal Gyrus	R	3.40	56	0	41	0.001
Frontal Superior Medial Gyrus	L	3.35	-14	29	35	0.001
Angular Gyrus	L	3.35	-41	-63	26	0.001
Crus Cerebellum II	L	3.33	-51	-54	-50	0.001
Supramarginal Gyrus	R	3.33	65	-23	45	0.001
Calcerine Sulcus	L	3.32	2	-99	0	0.001
Calcerine Sulcus	L	3.31	3	-99	9	0.001
Middle Temporal Gyrus	R	3.30	63	-62	8	0.001
Middle Temporal Gyrus	L	3.30	-63	-57	17	0.001
Middle Cingulate Cortex	R	3.28	6	21	39	0.001
Calcerine	L	3.27	3	-96	-8	0.001
Lingual Gyrus	R	3.26	20	-63	-6	0.001
Superior Parietal Lobule	L	3.26	-32	-53	66	0.001
Superior Frontal Gyrus	R	3.25	21	69	9	0.001
Supramarginal Gyrus	R	3.24	63	-32	29	0.001
Posterior Cingulate Cortex	R	3.23	8	-41	30	0.001
Superior Frontal Gyrus	L	3.23	-27	42	39	0.001
Inferior Occipital Gyrus	L	3.21	-21	-93	-12	0.001
Middle Temporal Gyrus	R	3.21	62	-63	5	0.001
Middle Cingulate Cortex	L	3.20	-9	-30	-35	0.001
Precuneus	R	3.20	14	-54	30	0.001

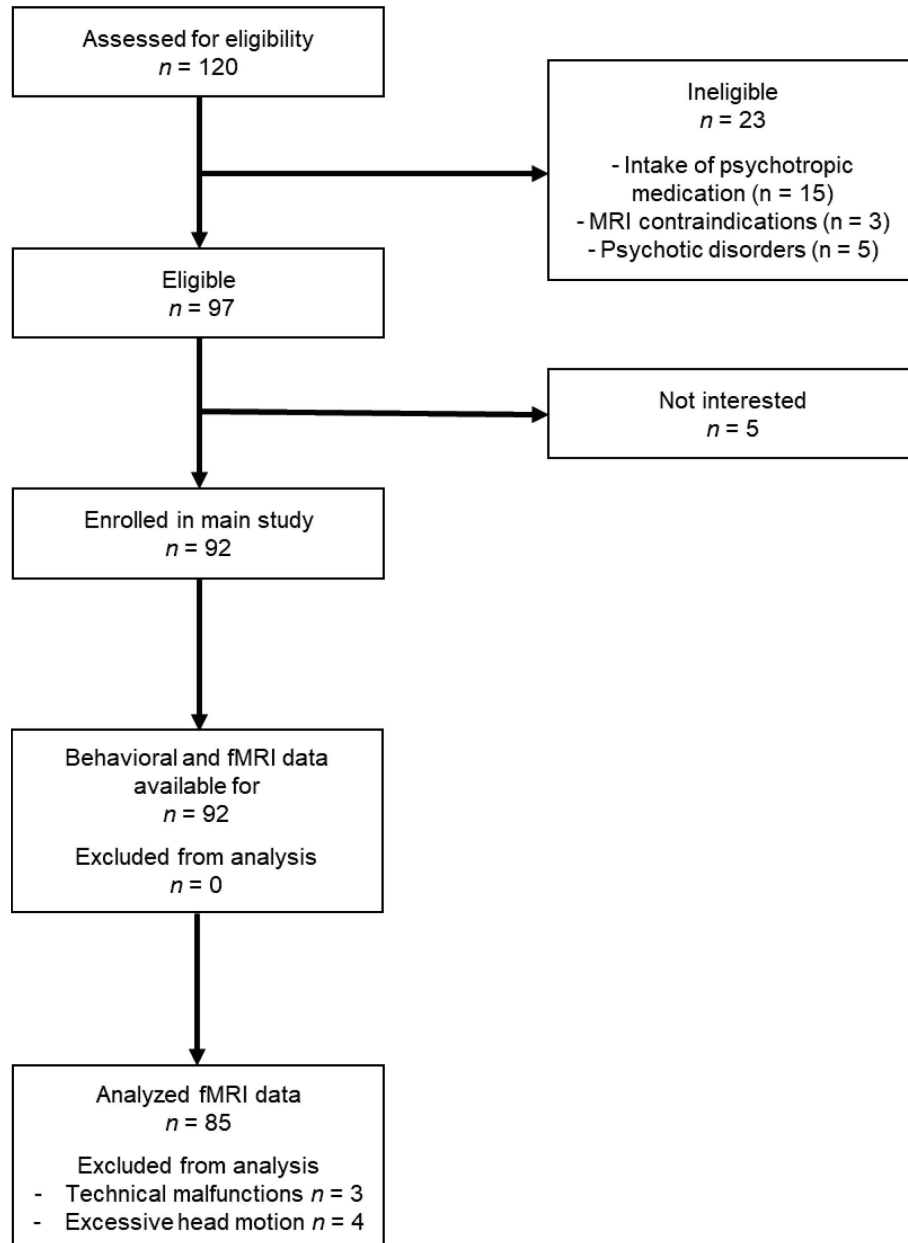
Low CM > Medium CM

Lobule IX of Vermis		4.26	2	-60	-41	<0.001
Superior Parietal Lobule	R	3.93	14	-56	63	<0.001
Cerebellum VIII	R	3.77	20	-57	-62	<0.001
Inferior Temporal Gyrus	L	3.68	-41	-38	-29	<0.001
Cerebellum VIIb	R	3.62	3	-77	-45	<0.001
Fusiform Gyrus	R	3.49	32	-2	53	<0.001
Superior Frontal Gyrus	L	3.21	-12	42	39	0.001

Notes. For the whole brain analysis a height threshold of $P < 0.001$ (uncorrected) was used. P -values are reported at peak level. Abbreviations: CM, childhood maltreatment.

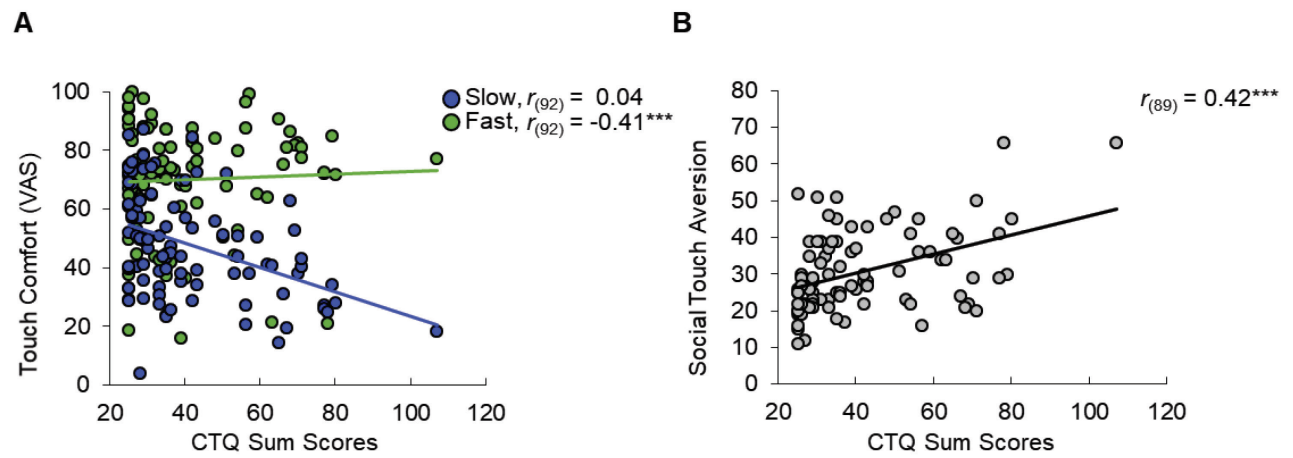
SUPPLEMENTAL FIGURES

Figure S1. Flow chart of participant recruitment



Participants were recruited from the local population by means of online advertisement and public postings. Subjects selected for study eligibility assessment had varying degrees of CM, which also included subjects with no reported history of CM. The final study sample consisted of 92 participants in the behavioral analysis. Due to technical malfunctions or excessive head motion ($> 3 \text{ mm/}^\circ$) during scanning, 7 participants had to be excluded from the fMRI analysis, leaving 85 participants for the fMRI analysis.

Figure S2. Associations between childhood trauma (CM) severity and the experience of social touch.



CM scores negatively correlate with comfort ratings of fast touch in an experimental paradigm **(A)** and positively correlate with general social touch aversion measured by a questionnaire **(B)**. Abbreviation: CTQ, Childhood Trauma Questionnaire. $^{***}P \leq 0.001$.

SUPPLEMENTAL REFERENCES

1. McGlone F, Olausson H, Boyle JA, et al: Touching and feeling: differences in pleasant touch processing between glabrous and hairy skin in humans. *Eur J Neurosci* 2012; 35:1782-1788
2. Kasper L, Bollmann S, Diaconescu AO, et al: The PhysIO Toolbox for Modeling Physiological Noise in fMRI Data. *J Neurosci Methods* 2017; 276:56-72
3. Glover GH, Li TQ, Ress D: Image-based method for retrospective correction of physiological motion effects in fMRI: RETROICOR. *Magn Reson Med Sci* 2000; 44:162-167
4. Harvey AK, Pattinson KT, Brooks JC, et al: Brainstem functional magnetic resonance imaging: disentangling signal from physiological noise. *J Magn Reson Imaging* 2008; 28:1337-1344
5. Birn RM, Smith MA, Jones TB, et al: The respiration response function: the temporal dynamics of fMRI signal fluctuations related to changes in respiration. *NeuroImage* 2008; 40:644-654
6. Mueller K, Lepsien J, Moller HE, et al: Cluster failure: Why fMRI inferences for spatial extent have inflated false-positive rates. *Front Hum Neurosci* 2017; 11:345
7. Tzourio-Mazoyer N, Landeau B, Papathanassiou D, et al: Automated anatomical labeling of activations in SPM using a macroscopic anatomical parcellation of the MNI MRI single-subject brain. *NeuroImage* 2002; 15:273-289
8. Ashburner J: A fast diffeomorphic image registration algorithm. *NeuroImage* 2007; 38:95-113
9. Dannlowski U, Stuhrmann A, Beutelmann V, et al: Limbic scars: long-term consequences of childhood maltreatment revealed by functional and structural magnetic resonance imaging. *Biol Psychiatry* 2012; 71:286-293
10. Lim L, Radua J, Rubia K: Gray matter abnormalities in childhood maltreatment: a voxel-wise meta-analysis. *Am J Psychiatry* 2014; 171:854-863
11. Hayes AF: Introduction to mediation, moderation, and conditional process analysis: A regression based approach. New York, NY, Guilford Press, 2013
12. Baron RM, Kenny DA: The moderator-mediator variable distinction in social psychological research: conceptual, strategic, and statistical considerations. *J Pers Soc Psychol* 1986; 51:1173-1182
13. Wittchen HU, Wunderlich U, Gruschwitz S, Zaudig M. Strukturiertes Klinisches Interview für DSM-IV [Structured clinical interview for DSM-IV]. Goettingen, Hogrefe, 1997
14. Weathers FW, Bovin MJ, Lee DJ, et al: The Clinician-Administered PTSD Scale for DSM-5 (CAPS-5): Development and initial psychometric evaluation in military veterans. *Psychol Assess* 2018; 30:383-395
15. Wilhelm FH, Kochar AS, Roth WT, Gross JJ: Social anxiety and response to touch: incongruence between self-evaluative and physiological reactions. *Biol Psychol* 2001; 58:181-202
16. Cohen S, Kamarck T, Mermelstein R: A global measure of perceived stress. *J Health Soc Behav* 1983; 24:385-396

17. Bernstein DP, Stein JA, Newcomb MD, et al. : Development and validation of a brief screening version of the Childhood Trauma Questionnaire. *Child Abuse Negl.* 2003;27:169-190
18. Iffland B, Brahler E, Neuner F, et al. Frequency of child maltreatment in a representative sample of the German population. *BMC Public Health.* 2013;13:980
19. Weathers FW, Bovin MJ, Lee DJ, et al. The Clinician-Administered PTSD Scale for DSM-5 (CAPS-5): Development and initial psychometric evaluation in military veterans. *Psychol Assess.* 2018;30:383-395
20. Steiger JH: Tests for comparing elements of a correlation matrix. *Psychol Bull* 1980;87:245-251